Enhancing Top-Emission OLED Performance Through the Introduction of Buffer Layers

Seung Ju Ok[1], Thi Na Le[1], JiHee Son[2], Seung Yong Song[2], and Min Chul Suh[1,]*
Department of Information Display, College of Sciences, Kyung Hee University, 26 [1]KyungheedaeRo, Dongdaemoon-Gu, Seoul 02447, Republic of Korea
[2]Display Research Center, Samsung Display Co., Ltd., Giheung 17113, Republic of Korea
Email: mcsuh@khu.ac.kr

Abstract

This study introduces a novel method to enhance top-emission OLED (TEOLED) performance using high-surface-energy metals, like aluminum, as buffer layers to control growth and achieve a smooth cathode surface. Optimization was further achieved by incorporating a bilayer electron injection layer with lithium fluoride (LiF), resulting in an 11.4% efficiency improvement and a 29% luminance increase.

1. Introduction

Organic Light-Emitting Diodes (OLEDs) have revolutionized the display industry by offering exceptional color purity, high contrast ratios, energy efficiency, and rapid response times. Among them, top-emission OLEDs (TEOLEDs) are widely employed in commercial displays, typically utilizing a cathode structure composed of silver (Ag) and magnesium (Mg). Since the introduction of the OLED structure by C.W. Tang in 1987, the Ag:Mg (10:1) cathode has become a standard due to its ability to achieve high efficiency through the microcavity effect [1-14]. However, this cathode configuration faces significant challenges, particularly in meeting the stringent requirements for extremely low sheet resistance in large-scale display panels [15]. Furthermore, the Ag:Mg cathode suffers from thermal instability issues, such as pixel shrinkage, which degrade display image quality.This degradation arises primarily from two factors: (1) Ag dewetting, caused by the high surface mobility and large surface energy disparity between the cathode and the underlying electron injection layer (EIL), leading to self-aggregation and island formation via Volmer-Weber growth, and (2) Mg diffusion, where the lightweight Mg migrates to the cathode surface, further exacerbating pixel shrinkage [15,16-17]. These issues are intensified by the low surface energy (γ) of conventional EIL materials, such as lithium fluoride (LiF, γ = 0.35 J/m²) [18-23]. To address these challenges, incorporating a high-surface-energy buffer layer between the cathode and EIL is essential to mitigate surface energy mismatches and suppress Ag dewetting. While significant efforts have been made to improve buffer layers, EILs, and cathode designs, achieving optimal device performance and thermal stability remains a critical challenge [24-25]. This study proposes an innovative strategy to overcome these limitations by introducing a high-surface-energy buffer layer between the cathode and the EIL. This approach effectively suppresses Ag dewetting and enhances thermal stability. By optimizing the EIL/buffer layer structure and adopting a pure Ag cathode, we achieved improved current efficiency compared to the reference device. Notably, under high-temperature conditions, the reference device exhibited pixel shrinkage, whereas the device with the buffer layer maintained robust pixel stability. This work underscores the pivotal role of buffer layers and cathode surface binding properties in enhancing the thermal stability and overall performance of TEOLEDs, offering valuable insights for advancing display technology.

2. Results and discussion

2.1. Factors contributing to cathode agglomeration.

Cathodes composed of Ag and Mg are widely utilized due to their excellent electron injection properties. However, this composition is prone to various challenges under harsh conditions, such as high temperatures. In particular, Mg exhibits a tendency to diffuse within interfaces or thin films, leading to morphological instability and ultimately compromising device performance.[26,27]

$$E_a = \frac{E_{bind}^2}{E_c} \quad (1)$$

Here, E_a represents the activation energy required for diffusion, E denotes the critical energy, and E_{bind} refers to the binding energy. The diffusion activation energy (E_a) is significantly influenced by the binding energy (E_{bind}) which serves as a critical factor in determining diffusion resistance.(Fig. 1a) In conventional Ag:Mg cathodes, the binding energy between Ag and Mg is relatively low, approximately 0.54 eV, resulting in increased metal atom diffusion and morphological instability in the thin film.(Fig. 1b) To overcome these limitations, approaches such as introducing buffer materials with higher binding energy to Ag or using pure Ag as the cathode material have been investigated. For instance, employing Al as a buffer layer significantly increases the binding energy between Al and Ag to 3.12 eV.(Fig. 1c) This enhanced binding energy reduces the diffusion coefficient of Ag atoms, thereby improving the thermal and structural stability of the cathode layer. Moreover, the binding energy between the buffer material and the electron injection layer (EIL) also plays a vital role in reinforcing the stability of the cathode structure. Through such material engineering approaches, the tendency for metal atom aggregation and diffusion can be effectively suppressed, enabling the realization of devices with high reliability and performance even under extreme conditions. This theoretical framework and experimental methodology underscore the importance of designing cathodes with optimal binding energy to achieve durable and high-performance devices.

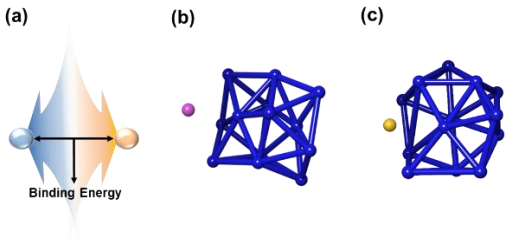

Figure 1. (a) Binding energy between atoms, (b) Ag and Mg, (c) Ag and Al.

2.2 Enhancing efficiency and thermal stability with buffer layer and bilayer EIL

Each material possesses a unique surface energy, which influences its interaction with water.(Table. 1) Higher surface

ISSN 0097-996X/25/5603-2213-$1.00 © 2025

energy results in stronger surface forces, causing DI-water to spread evenly upon contact. Conversely, lower surface energy weakens the attraction, leading to dewetting and water droplet aggregation.(Fig. 2a,2b) In this study, the EIL (LiF) exhibited a very low surface energy of 0.35 J/m², which reduced its binding energy with Ag and weakened adhesion. This, in turn, resulted in the formation of a rough cathode film with large particle sizes and surface irregularities, posing a significant challenge to achieving an optimal cathode structure. To address this issue, aluminum (Al), a material with higher surface energy, was introduced as a thin buffer layer (0.6 nm) to improve wettability during the cathode deposition process. To evaluate the changes in wettability, DI-water was dropped onto thin films of LiF, Ag, and Al, and their contact angles were measured. LiF showed the highest contact angle of 78°, indicating severe dewetting.(Fig. 2c) In contrast, Ag and Al exhibited similar contact angles, suggesting that both materials have comparable surface energies.(Fig. 2d,2e) demonstrate that the introduction of aluminum effectively enhanced the wettability of the cathode thin film, leading to the formation of a more uniform structure.[28]

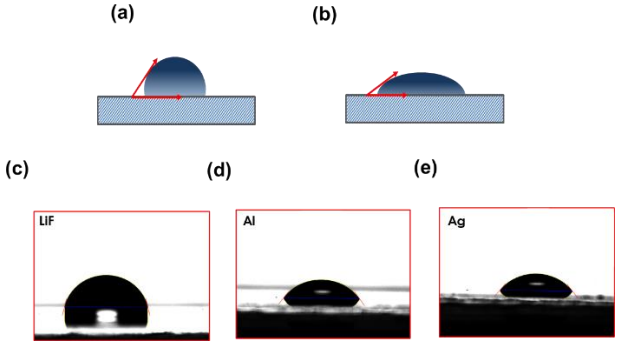

Figure 2. (a) Low surface energy, (b) High surface energy, (c) Contact angle of LiF, (d) Contact angle of Al, (e) Contact angle of Ag.

Table 1. Contact angles and surface energy of materials.

Thin films with significant surface energy differences are prone to Volmer-Weber growth, which serves as a major factor destabilizing cathode film formation (Figure 3-a). Volmer-Weber growth occurs when the film grows in the form of isolated particles rather than spreading uniformly across the substrate. This growth mechanism compromises the uniformity and stability of the thin film. In this study, efforts were directed toward suppressing Volmer-Weber growth and promoting Frank-Van der Merwe growth to achieve a more stable thin film formation (Figure 3-c). Frank-Van der Merwe growth involves the layer-by-layer formation of thin films on the substrate, resulting in uniform and stable film structures with superior physical properties, making it an ideal growth mode. By reducing surface energy differences and precisely controlling the growth process, this study presents an effective approach for fabricating stable and uniform cathode thin films. Such advancements are expected to play a critical role in enhancing OLED performance.[29]

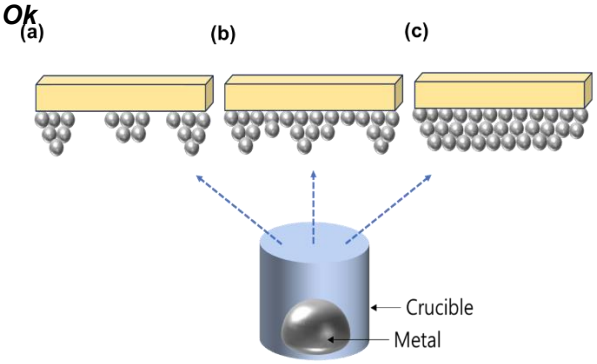

Figure 3. Types of film growth (a) Volmer-Weber, (b) Stranski-Krastanov, (c) Frank-Van der Merwe.

Based on theoretical insights, scanning electron microscopy (SEM) analysis was conducted on thin films of Ag deposited on LiF and samples incorporating an Al buffer layer between the EIL and the cathode. The results revealed that samples with the Al buffer layer exhibited significantly smoother surfaces, highlighting the crucial role of such buffer layers in enhancing the stability and performance of the device (Fig. 4a,4b).Notably, Al facilitates the effective release of lithium ions (Li^+) through a chemical reaction with LiF. The released Li^+ ions migrate into the ETL layer, where they act as n-dopants, shifting the Fermi level closer to the LUMO level of the ETL at the interface.(Fig. 4c,4d) This process reduces the electron injection barrier, thereby substantially improving the electrical performance of the device.Additionally, the Al buffer layer enhances wettability, effectively minimizing surface cracks and roughness during the deposition process. These improvements enable the formation of a more uniform and stable cathode thin film, which ultimately contributes to better overall OLED performance. These findings demonstrate that the Al buffer layer serves as a multifunctional material capable of simultaneously improving both physical and electrical properties. Utilizing such a buffer layer in cathode design presents a promising strategy for optimizing the efficiency and stability of OLED devices.

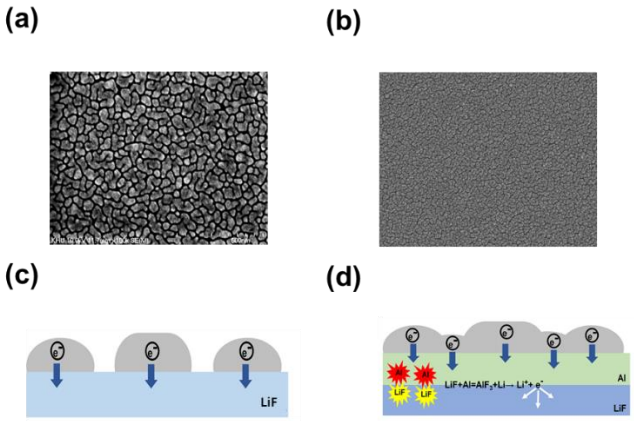

Figure 4. (a) Surface image of LiF-Ag, (b) Surface image of LiF-Al-Ag, (c) Electron injection in Volmer-Weber mode, (d) Electron injection with Al insertion

Performance testing of the fabricated devices revealed that the conventional device with a single LiF EIL exhibited a maximum current efficiency of 116.1 cd/A and a power efficiency of 104 lm/W. In contrast, the device incorporating an Al buffer layer demonstrated significantly improved performance, achieving a current efficiency of 131 cd/A and a power efficiency of 117 lm/W, along with higher luminance and overall efficiency (Fig. 5b-5d, Table 2).This enhancement in performance can be attributed to the introduction of the Al buffer layer, which improved the chemical stability of the interface and facilitated more uniform and stable contact due to Al's high surface energy.

The Al buffer layer promoted the release of lithium ions (Li^+) through a chemical reaction with LiF, enhancing electron injection into the ETL layer and optimizing the electronic properties of the interface. Additionally, Al improved wettability, effectively reducing surface roughness and cracks during the thin-film deposition process, thereby increasing the physical stability of the device.In conclusion, the Al buffer layer significantly enhanced the current efficiency, power efficiency, and luminance of OLED devices, establishing itself as a crucial and practical design element for achieving high-performance OLEDs.

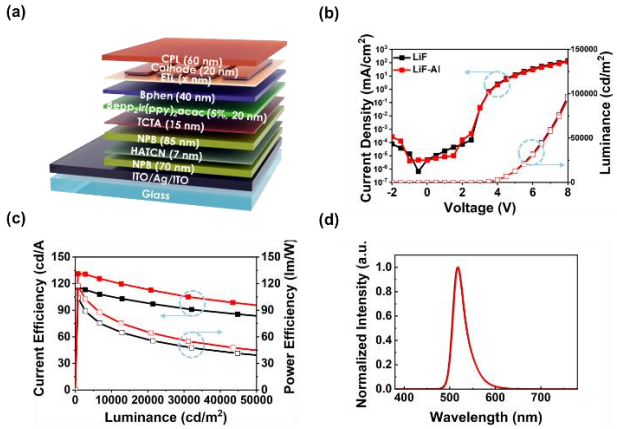

Figure 5. (a) Device Struature, (b) Current density –voltage - luminance, (c) Current efficiency – luminance - Power efficiency, (d) EL spectrum.

Table 2. Device characteristics of TEOLEDs with single LiF and those incorporating Al.

Device	V_{on} (V)	*Luminance* (@8Vcd/m²)	*C.E.* (cd/A) @MAX	*P.E.* (lm/W) @MAX	λ_{max} (nm)	*FWHM* (nm)
LiF	3.5	155,528	116	104	518	29
LiF/Al	3.5	220,005	131	117	518	29

3. Conclusion

Top-emission organic light-emitting diodes (TEOLEDs) face a critical challenge under thermal stress conditions. This issue arises from the intrinsic properties of silver (Ag), characterized by high surface energy and atomic mobility. These properties, coupled with the substantial surface energy disparity between the cathode and the electron injection layer (EIL), trigger the Volmer–Weber growth mechanism, resulting in self-aggregation and degraded device performance. Additionally, the low binding energy (*E*bind) between metal atoms accelerates thermal diffusion, exacerbating morphological instability and ultimately causing pixel shrinkage. To address this challenge, this study introduces a strategic approach involving the incorporation of a buffer layer to enhance thermal stability and device efficiency. By combining Ag with materials possessing relatively high *E*bind, the uniformity of the cathode thin film was significantly improved. Furthermore, high-surface-energy metals were employed as buffer layers to optimize the growth mechanism, enabling the formation of smooth and stable cathode thin films. As a result, the TEOLEDs achieved up to an 11.4% increase in efficiency and a 29% enhancement in luminance. Future research will focus on deepening the understanding and generalization of the thermal stability mechanisms in the proposed TEOLEDs through computational modeling techniques such as molecular dynamics simulations. These studies aim to investigate atomic-scale thermal diffusion processes in the materials studied, providing valuable insights into the interplay between material properties and device performance under thermal stress.

4. Impact of Your Research

This study presents a significant breakthrough in improving the thermal stability and device performance of top-emission OLEDs (TEOLEDs). By effectively addressing issues caused by thermal stress, it greatly enhances the durability and reliability of displays, thereby expanding their commercial viability. Furthermore, the innovative approach of introducing high-surface-energy buffer layers overcomes the limitations of existing technologies, establishing a new benchmark for efficient and stable cathode design. These advancements not only enable superior performance and stability in large-scale and high-resolution OLED technologies but also open up possibilities for application in various electronic devices facing similar thermal stability challenges, contributing broadly to advancements across related fields.

5. Acknowledgements

This study was supported by Samsung Display. It was also supported by the Basic Science Research Program through the NRF, by the Ministry of Science and ICT, Korea(2021R1A2C1008725), and the Industrial Strategic Technology Development Program (RS2024-00417913, RS-2024-00418116, 20011059, 20014668), funded through KEIT, by the Ministry of Trade, Industry and Energy, Korea.

6. References

1. Tang, Ching W., and Steven A. VanSlyke, Organic electroluminescent diodes, Appl. Phys.Lett. 1987, 51, 913-915.
2. J. H. Kim, J.-Y. Lee, C. Lim, J. Roh, S.-W. Baek, W. Kim, M. C. Suh, H. Yu, Adv. Funct.Mater. 2023, 33, 2214530.
3. J.-X. Man, S.-J. He, D.-K. Wang, H.-N. Yang, Z.-H. Lu, Org. Electron. 2018, 63, 41–46.
4. R. Vladoiu, A. Mandes, V. Dinca, P. Kudrna, M. Tichý, S. Polosan, Jalloy Compd. 2021,869, 159364.
5. B. Pyo, C. W. Joo, H. S. Kim, B. H. Kwon, J. I. Lee, J. Lee, M. C. Suh, Nanoscale. 2016,8(16), 8575-8582.
6. N. S. Kim, W. Y. Lee, B. Pyo, M. C. Suh, Org. Electron. 2017, 44, 232-237.
7. S. R. Park, M. C. Suh, Opt. Express. 2018, 26(4), 4979-4988.
8. H. Cho, C. M. Kang, S. Choi, C. W. Joo, B. H. Kwon, J. W. Shin, N. S. Cho, J. Inf. Display.2024, 25(3), 261-269.
9. N. S. Kim, S. H. Jung, M. C. Suh, J. Soc. Inf. Display. 2018 26(2), 79-84.
10. M. C. Suh, D. Y. Kim, S. H. Jung, N. S. Kim, Org. Electron. 2020, 77, 105493.
11. B. Sung, C. W. Joo, J. C. Yang, A. Gasonoo, S. W. Woo, J. H. Lee, J. Lee, J. Inf. Display.2023, 24(1), 71-79.
12. N. S. Kim, D. Y. Kim, J. H. Song, M. C. Suh, Opt. Express. 2020, 28(21), 31686-31699.
13. J. H. Kim, J. Y. Lee, C. Lim, J. Roh, S. W. Baek, W. Kim, H. Yu, Adv. Funct. Mater. 2023,33(20), 2214530.
14. J. Roh, A. Nimbalkar, M. C. Suh, ACS Photonics. 2024, 11, 4606–4615.
15. S. K. Kwon, E. H. Lee, K. S. Kim, H. C. Choi, M. J. Park, S. K. Kim, J. H. Kwon, Opt.Express. 2017, 25, 29906-29915.
16. E. Baeur, J.H. van der Merwe, Phys. Rev. B. 1986, 33, 3657–3671.

17. G. Abadias, L. Simonot, J.J. Colin, A. Michel, S. Camelio, D. Babonneau, Appl. Phys. Lett.2015, 107, 183105.
18. L. Vitos, A.V. Ruban, H.L. Skriver, J. Kolla´r, Surf. Sci. 1998, 411, 186–202.
19. X. Yang, P. Gao, Z. Yang, J. Zhu, F. Huang, J. Ye, Sci. Rep. 2017, 7, 44576-44584.
20. D. Gall, J. Appl. Phys. 2016, 119, 0851011-0851015.
21. M. E. Callow and R. L. Fletcher, Int. Biodeterior. Biodegrad. 1994, 34, 333-348.
22. Z. Li, L. Zhang, H. Xue, H. Yang, Y. Yu, L. Xu, Y. Li, J. Peng, Org. Electron. 2022, 103,106468.
23. T. N. Le, R. Elumalai, S. J. Ok , Y. Lee, S. Y. Song, M. C. Suh, Org. Electron. 2024, 130,107061.
24. M.-G. Song, K.-S. Kim, H. I. Yang, S. K. Kim, J.-H. Kim, C.-W. Han, H.-C. Choi, R. Pode,J. H. Kwon, Org. Electron. 2020, 76, 105418.
25. S. K. Kim, R. Lampande, and J. H. Kwon, ACS Photonics. 2019, 6 (11), 2957-2965.
26. T. Kaub, R. Anthony, G. B. Thompson, J. Appl. Phys. 2017, 122, 22.
27. Banerjea, A., & Smith, J. R, Phys. Rev. B. 1988, 37.12:6632.
28. H. Heil, J. Steiger, S. Karg, M. Gastel, H. Ortner, H. V. Seggern & M. Stößel, J. Appl. Phys. 2001, 89, 420-424.
29. P.-C. Kao; J.-H.Lin; J.-Y. Wang; C.-H. Yang; S.-H. Chen, Appl. Phys. 2011, 109